J IRAN CHEM SOC
DOI 10.1007/s13738-016-1007-7

ORIGINAL PAPER

PEDOT nanofiber/Pd(0) composite-mediated aqueous Mizoroki–Heck reactions under ultrasonic irradiation: an efficient and green method for the C–C cross-coupling reactions

Seyed Jamal Tabatabaei Rezaei[1]

Received: 2 June 2016 / Accepted: 2 November 2016

Abstract An environmentally benign and highly efficient procedure for the C–C cross-coupling reactions of aryl halides with olefinic compounds has been developed under ultrasonic irradiation in water in the presence of PEDOT nanofibers/Pd(0) composites (PEDOT-NFs@Pd) as a new recyclable catalyst. PEDOT-NFs@Pd catalyzed the reaction efficiently without using any other harmful organic ligands. Cleaner reaction profile, easy workup procedure, high yields and short reaction time duration are some remarkable features of this method. The utilization of ultrasound irradiation offers a fast, clean and versatile synthetic tool that is often unavailable by conventional methods. Moreover, the catalyst can be recovered by simple filtration and reused several times without significant loss of activity.

Electronic supplementary material The online version of this article (doi:10.1007/s13738-016-1007-7) contains supplementary material, which is available to authorized users.

✉ Seyed Jamal Tabatabaei Rezaei
sjt.rezaei@znu.ac.ir

[1] Department of Chemistry, Faculty of Science, University of Zanjan, P.O. Box 45195-313, Zanjan, Iran

Published online: 08 November 2016

Graphical Abstract

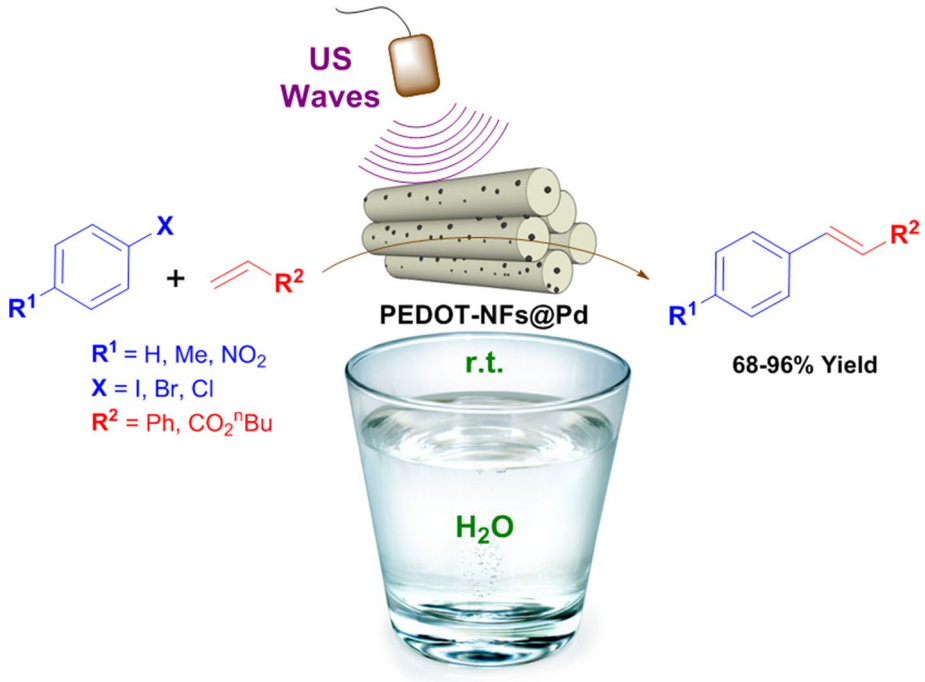

Keywords PEDOT nanofibers · Palladium · Recyclable catalyst · Aqueous Heck reaction · Ultrasonic irradiation

Introduction

With the increasing environmental awareness in chemical research, the challenge of designing sustainable environmentally friendly procedures has become the fundamental goal of green chemistry [1]. Ultrasound-assisted organic transformation is a promisingly useful approach to a green technique in organic chemistry. In the last few years, the use of ultrasound irradiation in organic synthesis became more and more interesting as ultrasonic waves in liquids are known to cause chemical reactions either in homogeneous or in heterogeneous systems [2–4]. In general, organic reactions under the ultrasound irradiation have many advantages compared to the conventional reactions which need very high temperatures. Ultrasound-assisted reactions are cleaner, last only very few minutes, have high yield and produce minimum waste [2, 4–7].

On the other hand, water has aroused considerable attention in synthetic community and proved to be a promising solvent in organic synthesis due to its economic, environmentally friendly and polar nature. In relation to this, significant efforts have been dedicated to developing organic reactions in water with many inherent advantages over reactions in conventional organic solvents [8–12].

The palladium-catalyzed Heck cross-coupling reaction between aryl halides and alkenes is a versatile method for carbon–carbon bond formation in synthetic organic chemistry [13, 14]. Palladium has been known as an indispensable catalyst for these cross-coupling reactions, and there is a great deal of literature on its properties in many reactions. Recently, supported palladium nanoparticles on insoluble solids have captured the attention of researchers worldwide as new generation of heterogeneous catalysts in various scientific fields due to their superior catalytic performance, good stability, ease of separation and satisfactory reusability compared to the traditional homogeneous $Pd(OAc)_2$, $PdCl_2$ catalysts [15–25]. The most commonly used supports are silica-based materials, magnetic nanoparticles, self-assembled monolayers, carbon nanomaterials, dendrimers and functional polymers [26–35].

Of the major conducting polymers, PEDOT has been widely studied because of its simple synthesis, high electrochemical stability and charge mobility, moderate band gap, low redox potential and wide range of applications [36–38]. Generally, supported metal nanoparticles are produced by chemical reduction of metal ions in the presence of a support. Commonly used reductants are borohydride, citrate, ascorbate and elemental hydrogen [39]. PEDOT, however, provides both stabilization and reducing properties. Due to the unique features of PEDOT, metal/PEDOT nanocomposites have been the subject of interest of several groups [40–43]. In general, metal nanoparticles are produced by adding a metal salt to an aqueous dispersion of PEDOT [44]. This

Scheme 1 Mizoroki–Heck cross-coupling reactions

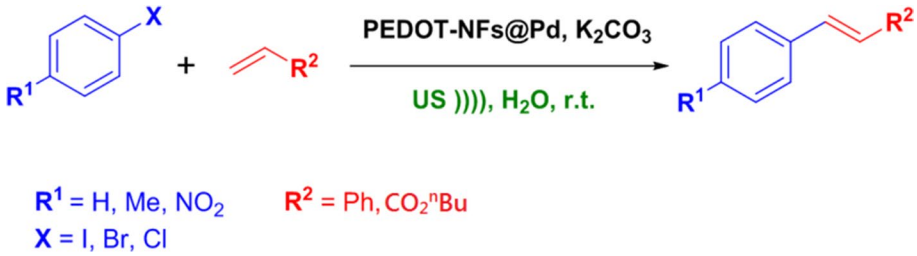

approach eliminated the need for a separate reduction reaction, which can reduce the spread of toxic reagents during extra chemical reactions. When rapidly initiated polymerization is used for the synthesis of polymer, PEDOT with nanofibrous morphology is formed [45, 46]. The high surface area and porosity of the PEDOT nanofibers serve as an ideal support to make metal/PEDOT nanocomposites [47–50].

To take advantage of these characteristics, in this work we have developed new methodology for the Heck cross-coupling reactions of aryl halides with olefinic compounds in the presence of PEDOT nanofibers/Pd(0) composites as a green and recyclable catalyst in a green solvent under ultrasound irradiation (Scheme 1).

Experimental

Apparatus and reagents

All solvents and reagents were purchased from Aldrich or Merck and used without further purification unless otherwise stated. Scanning electron microscopy (SEM) is performed by field emission scanning electron microscopy of Philips XL-30 instrument with the operation of 17 kV. Transmission electron microscopy (TEM) analyses were performed by LEO 912AB electron microscope. The content of Pd in the PEDOT nanofibers/Pd composite was determined by AA-680 Shimadzu (Kyoto, Japan) flame atomic absorption spectrometer (AAS) and thermogravimetric analysis (TGA) (STA 1500 instrument at a heating rate of 10 °C min^{-1} in air). IR spectra were recorded on a Bomem MB-Series FT-IR spectrophotometer. Catalysis products were analyzed using a Varian 3900 GC (GC conversions obtained using n-decane as an internal standard and are based on the amount of aryl halide employed in relation to authentic standard product). ^{1}H and ^{13}C NMR spectra ($CDCl_3$) were recorded on a BRUKER DRX-250 AVANCE spectrometer at 250.0 and 62.5 MHz, respectively. X-ray powder diffraction (XRD) data were collected on an XD-3A diffractometer using Cu Kα radiation. The average size of crystallites was calculated from the peak broad (111) by using the Debye–Scherrer equation [51]. XPS analysis was performed using a VG Multilab 2000 spectrometer (Thermo VG scientific) in an ultra-high vacuum. The sonication was performed in a UP 400S ultrasonic processor equipped with a 3-mm-wide and 140-mm-long probe, which was immersed directly into the reaction mixture. The operating frequency was 24 kHz, and the output power was 0–400 Watts through manual adjustment. Ultrasonic bath (EUROSONIC® 4D ultrasound cleaner with a frequency of 50 kHz and an output power of 350 W) was used to disperse materials in solvents.

Preparation of PEDOT nanofibers/Pd composites (PEDOT-NFs@Pd)

PEDOT nanofibers/Pd composite was prepared by first synthesizing PEDOT nanofibers in a rapidly initiated polymerization reaction [43, 44]. Briefly, 1.5 mmol 3,4-ethylenedioxythiophene (EDOT) was dispersed in 90 mL HCl (1.0 M) under ultrasonic stirring for 10 min. Then, 10 mL acid solution (HCl, 1.0 M) of $FeCl_3$ (0.75 mmol) was added into the above mixture quickly and immediately shaking to ensure sufficient mixing before polymerization begins. The polymerization reaction was carried out at 20 °C for 22 h without any disturbance. The synthesized PEDOT-NFs precipitate was obtained through centrifugation and then washed with deionized water several times to remove the redundant dopant and oxidant. Finally, the dark-blue product was obtained after being dried in vacuum at 60 °C for 24 h. Palladium nanoparticles were grown by combining a aqueous solution of PEDOT nanofiber (10 mL, 0.002 g mL^{-1}) with a 10 mM solution of palladium(II) nitrate (2.15 mL) and incubation for one day. The resulting solution was then dialyzed to remove any remaining palladium salt in fresh deionized water every 4 h for 2 days. AAS analyses of the filtrates after dialysis showed no palladium.

General procedure for the catalytic tests

A mixture of an aryl halide (1.0 mmol), an alkene (*n*-butyl acrylate or styrene) (1 mmol), K_2CO_3 (1.2 mmol) and PEDOT-NFs@Pd (96 mg, 0.05 mol% of Pd with respect to aryl halide) in water (3 mL) was exposed to ultrasonic irradiation at 170 W at the room temperature for a specified length of time. The reaction was monitored by TLC (or GC if necessary). After the completion of the reaction,

the catalyst was collected by simple filtration, washed several times with absolute ethanol, air-dried and used directly for the next round of reactions without further purification. After separation of the catalyst, the collected solution was poured into water and extracted with CH_2Cl_2. The combined organic phases were dried over Na_2SO_4, filtered and evaporated in vacuum. The mixture was then purified by column chromatography over silica gel (eluent: ethyl acetate/petroleum ether, 1/4) or recrystallization to afford a product with high purity. Characterizations of the products were performed by comparison with their ^{1}H-NMR, ^{13}C-NMR and physical data with those of authentic samples.

Results and discussion

Characterization of the supported catalyst

The chemical structure of the PEDOT nanofibers was characterized by FT-IR spectroscopy. A typical FT-IR spectrum is shown in Fig. 1; it is in good agreement with the previously reported results [44]. The vibrations at 1340 and 1515 cm^{-1} are due to the C–C or C=C stretching of the quinoidal structure of thiophene ring and the ring stretching of thiophene ring, respectively. The peaks originating from the stretching in the alkylenedioxy group are observed at 1210 and 1088 cm^{-1}. The peaks assigned to C–S bond stretching in the thiophene ring are also observed at 980, 815 and 682 cm^{-1}. The presence of the peak at 1650 cm^{-1} in the FT-IR spectrum indicates the existence of an over-oxidized carbonyl group [44].

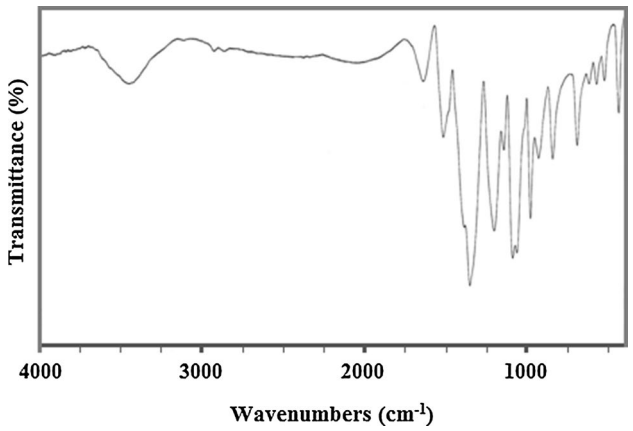

Fig. 1 FT-IR spectrum of PEDOT-NFs

Figure 2a shows the SEM image of the PEDOT nanofibers. The PEDOT nanofibers are clearly evident in the SEM image with a length of more than 10 μm and diameters in the range of 250–500 nm. TEM experiments demonstrate that palladium nanoparticles were uniformly dispersed on the surface of PEDOT-NFs (Fig. 2b). This is due to the existence of a large number of sulfur and oxygen heteroatoms, as anchoring sites, on the surface of PEDOT-NFs (Fig. 3) [37].

The XRD patterns for the PEDOT-NFs@Pd show the expected crystallinity of Pd(0) nanoparticles and fibrous PEDOT (Fig. 4). Three broad peaks centered at $2\theta = 6.5°$, 12.8° and 26.8° and an intense sharp peak at $2\theta = 8.9°$ are observed in the PEDOT-NFs oxidized by $FeCl_3$ [44]. The other three peaks of PEDOT-NFs@Pd are characteristics of face-centered cubic (fcc) crystalline Pd, corresponding to the planes (1 1 1), (2 0 0) and (2 2 0) at 2θ values of about 40.02, 46.59 and 68.03, respectively. The average particle size has been calculated using Scherrer's formula according to the broadening of the (1 1 1) characteristic peak of the XRD pattern. Accordingly, the average particle size of Pd is 19.6 nm.

The surface composition and chemical oxidation states of the prepared PEDOT-NFs@Pd catalyst were characterized by XPS. Wide XPS scan from PEDOT-NFs@Pd (Fig. 5a) shows the presence of Pd 3*d* signal together with S 2*p*, C 1*s* and O 1*s* signals derived from PEDOT-NFs. Thus, the XPS data also confirm the presence of Pd in the

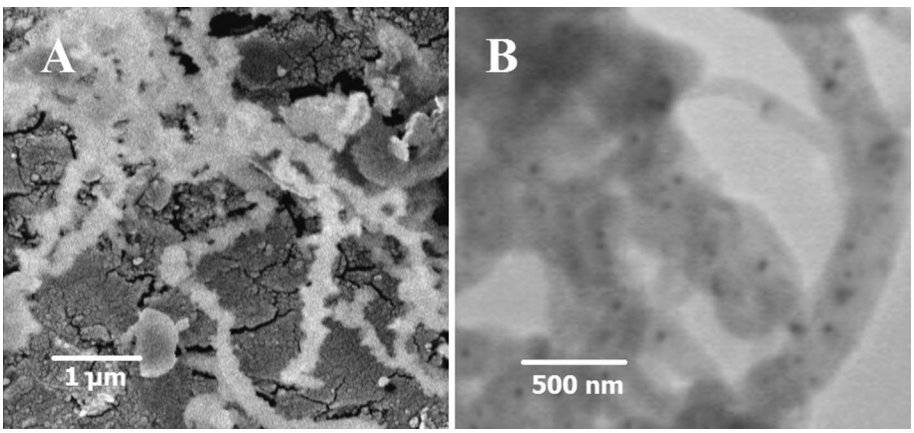

Fig. 2 SEM image of PEDOT-NFs (**a**) and TEM image of PEDOT-NFs@Pd (**b**)

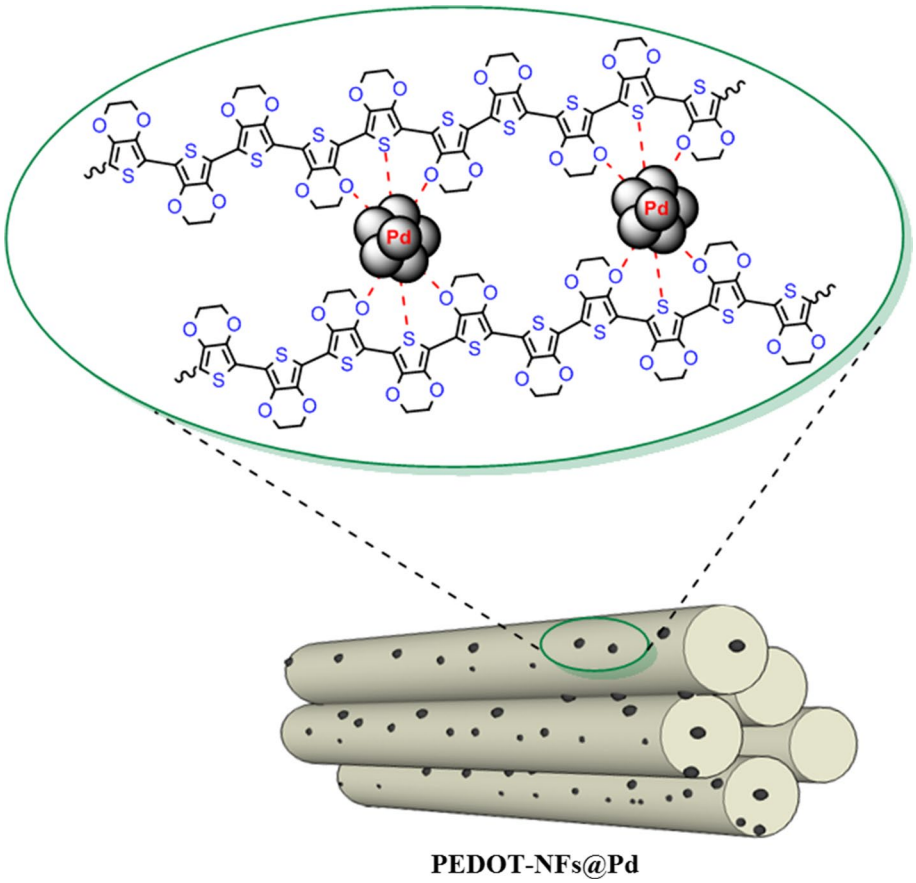

Fig. 3 The molecular structure of the PEDOT chains forming PEDOT-NFs@Pd

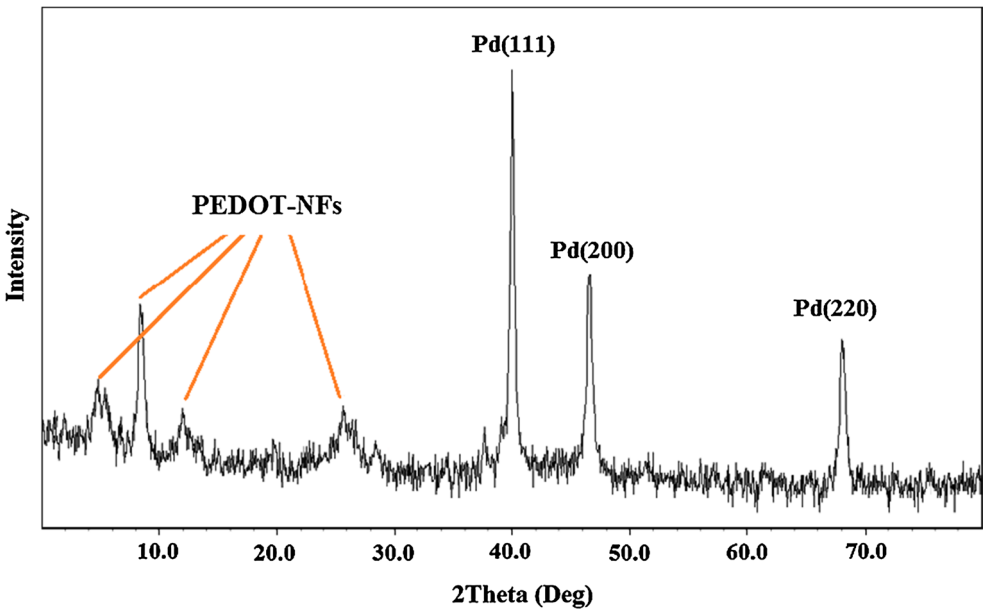

Fig. 4 XRD pattern of PEDOT-NFs@Pd

prepared PEDOT-NFs@Pd catalyst. The high-resolution Pd 3*d* XPS spectrum of PEDOT-NFs@Pd is illustrated in Fig. 5b which reveals the presence of Pd $3d_{5/2}$ and $3d_{3/2}$ peaks at binding energies of 335.4 and 340.85 eV, respectively. These results are consistent with those reported for metallic Pd(0) oxidation state [48–50, 52]. Also, the

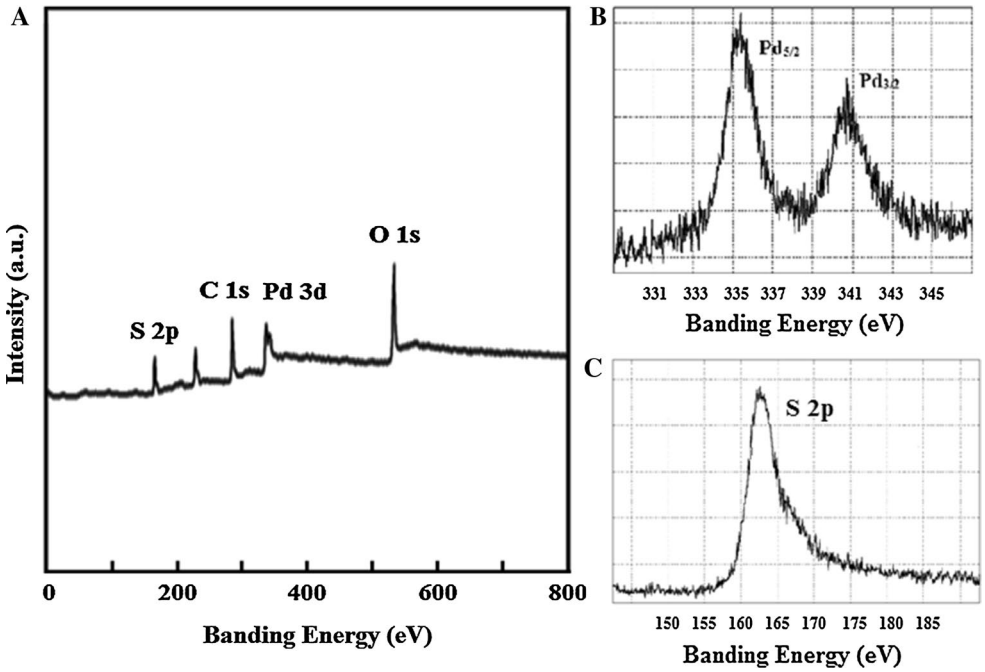

Fig. 5 XPS survey spectrum of PEDOT-NFs@Pd (**a**). High-resolution Pd 3d (**b**) and S 2p (**c**) XPS spectra of PEDOT-NFs@Pd

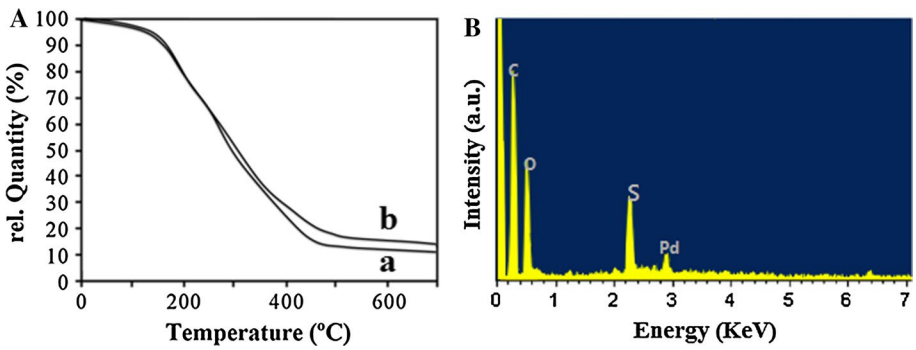

Fig. 6 TGA curves of PEDOT-NFs (**A**-*a*) and PEDOT-NFs@Pd (**A**-*b*). EDS spectrum of PEDOT-NFs@Pd (**B**)

high-resolution S 2*p* spectrum of PEDOT-NFs@Pd is illustrated in Fig. 5c which correspond to the single sulfur bonding environment in PEDOT.

The AAS technique was used to calculate the weight percent of palladium in catalyst. The data showed that the amount of palladium immobilized on PEDOT-NFs is about 5.51 wt%. The actual weight loss corresponding to the combustion of supported hybrid material was determined by thermogravimetry as the weight loss between 100 and 700 °C, i.e., excluding the weight loss due to the desorption of water (Fig. 6A). Comparing the two curves demonstrates that the weight percent of palladium in synthesized catalyst is about 5.55% which is consistent with the obtained results by the AAS technique. Also, energy-dispersive X-ray spectroscopy (EDS) analysis of the catalyst directly confirmed the presence of Pd in the catalyst structure (Fig. 6B). The EDS spectrum of PEDOT-NFs@Pd shows the elements C, O, S and Pd with wt% of 48.38, 22.01, 21.73 and 5.12, respectively.

The Catalytic activity of PEDOT-NFs@Pd toward the Heck cross-coupling reactions

To evaluate the catalytic properties of this catalyst, various bases, solvents, catalyst amounts and the output power of the ultrasound apparatus were employed in a model Heck coupling reaction between 4-methyl-iodobenzene and n-butyl acrylate and the conversion yields were measured by GC.

Initially, the reaction was carried out in the presence of various solvents and bases. As shown in Tables 1 and 2, water and K_2CO_3 were the best solvent and base for this synthesis, respectively. Other solvents and bases gave only moderate yields of the product (Tables 1, 2).

Since the effect of solvent and base was optimized, the influence of the amounts of catalyst on the reaction was studied in the next step (Table 3). At very low catalyst loading, the reaction required long duration to get completed even under harsh thermal conditions (Table 3, entry

Table 1 Effect of different solvents on the reaction of 4-methyl-iodobenzene and n-butyl acrylate

Entry	Solvent	Conversion (%)
1	DMF	92
2	THF	20
3	CH_3CN	45
4	Toluene	53
5	H_2O	99

Reaction conditions: 1 mmol 4-methyl-iodobenzene, 1 mmol *n*-butyl acrylate, 1.2 mmol K_2CO_3, PEDOT-NFs@Pd (0.05 mol% Pd) and US power: 170 W at room temperature for 25 min

Table 2 Effect of different bases on the reaction of 4-methyl-iodobenzene and n-butyl acrylate

Entry	Base	Conversion (%)
1	None	Trace
2	Et_3N	91
3	K_2CO_3	99
4	NaOAc	88
5	$CsCO_3$	67

Reaction conditions: 1 mmol 4-methyl-iodobenzene, 1 mmol *n*-butyl acrylate, 3 mL water, PEDOT-NFs@Pd (0.05 mol% Pd) and US power: 170 W at room temperature for 25 min

Table 3 Influence of the amount of catalyst on coupling reaction of 4-methyl-iodobenzene with n-butyl acrylate

Entry	Amount of catalyst (mol% Pd)	Temp. (°C)	Conversion (%)
1	0.001	r.t.	17
2	0.001	80	26
3	0.01	r.t.	75
4	0.05	r.t.	99
5	0.1	r.t.	99

Reaction conditions: 1 mmol 4-methyl-iodobenzene, 1 mmol *n*-butyl acrylate, 1.2 mmol K_2CO_3, 3 mL water and US power: 170 W for 25 min

1 and 2). As the catalyst amount was increased (0.05 mol% Pd with respect to 4-methyl-iodobenzene), the reaction went to completion more rapidly at room temperature. It was found that the best system was water as solvent and K_2CO_3 as base using 0.05 mol% of catalyst at room temperature.

We also found that the output power of the ultrasound apparatus greatly affected this transformation. The obvious improvement in the conversion (99%) reached a plateau

Table 4 Effect of sonication power on the reaction of 4-methyl-iodobenzene and n-butyl acrylate

Entry	US power (W)	Time (min)	Conversion (%)
1	120	25	68
2	120	60	71
3	140	25	87
4	170	25	99
5	200	25	99
6	–	120	90[a]
7	–	240	92[a]

Reaction conditions: 1 mmol 4-methyl-iodobenzene, 1 mmol *n*-butyl acrylate, 1.2 mmol K_2CO_3, 3 mL water and PEDOT-NFs@Pd (0.05 mol% Pd) at room temperature

[a] Reaction temperature (90 °C)

at 170 W of power. Using higher acoustic power did not change reaction yield a considerable amount (99% in the same time), but using lower power sharply decreased the conversion to approximately 71% even with more reaction time (Table 4, entry 2). These facts mean that there is an optimum power for effective Heck reaction. The similar ultrasound power effect is observed for several other reactions [7, 11, 53–55].

In order to verify the effect of ultrasound irradiation on this transformation, we also examined this reaction under thermal conditions (Table 4, entry 6 and 7). Analysis of the reactions mixture showed that reaction takes place efficiently at 90 °C for 2 h. It is apparent that the coupling reaction can be finished in shorter time to get better yields under ultrasound irradiation.

In order to prove the catalytic applicability of PEDOT-NFs@Pd, we studied the Heck coupling reactions of styrene and n-butyl acrylate with different aryl halides under similar conditions (Scheme 1; Table 5). The results show that various aryl bromide or iodide bearing either electron-withdrawing or electron-donating groups (Table 5, entries 1–10) could be efficiently converted to the corresponding coupling products in high yields under optimum condition. Furthermore, as shown in Table 5 (entries 11–16) the catalytic amount of PEDOT-NFs@Pd can be used in the Heck coupling of even less reactive aryl chloride derivatives in good yields with an increase in the reaction time as the electron-donating properties of substituents increase.

For practical applications of heterogeneous catalysts, especially in industry, the heterogeneity and level of reusability are very important. To address these issues, the stability and reusability of the PEDOT-NFs@Pd catalyst was studied for the Heck cross-coupling reaction of

Table 5 Heck reaction of styrene and n-butyl acrylate with different aryl halides

Entry	R^1ArX	R^2	Time (min)	Yield (%)[a]
1		Ph	18	93
2		CO_2Bu	15	96
3	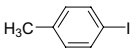	Ph	35	91
4	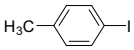	CO_2Bu	25	95
5	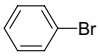	Ph	40	89
6	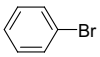	CO_2Bu	35	92
7	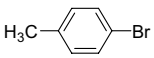	Ph	45	90
8	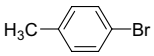	CO_2Bu	40	92
9	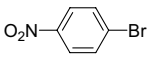	Ph	20	94
10	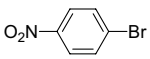	CO_2Bu	15	95
11	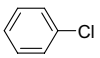	Ph	60	71
12	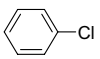	CO_2Bu	60	83
13	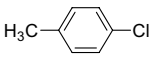	Ph	75	68
14	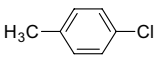	CO_2Bu	60	77
15	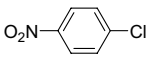	Ph	45	88
16	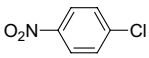	CO_2Bu	45	91

Reaction conditions: 1 mmol R^1ArX, 1 mmol olefin, 1.2 mmol K_2CO_3, 3 mL water, PEDOT-NFs@Pd (0.05 mol% Pd) and US power: 170 W at room temperature

[a] Isolated yield of pure product

4-methyl-iodobenzene with n-butyl acrylate in optimum condition up to six cycles. After each experimental run, the reaction products were extracted into CH_2Cl_2 followed by a simple decantation and subsequently the conversion of product was determined by means of GC. Also, the filtered catalyst washed several times with absolute ethanol, air-dried and used directly for the next round of reactions. The results shown in Fig. 7 demonstrate that the recovered catalyst had not significantly lost its activity after six cycles, clearly illustrating the high stability and excellent reusability of the catalyst. Also, the amount of leached Pd species in the reaction solution was measured by the AAS technique. The amount of palladium leaching after the first and last run was determined by AAS analysis to be only 0.01 and 0.3%, respectively. Therefore, we may conclude that the observed catalysis is truly heterogeneous in nature.

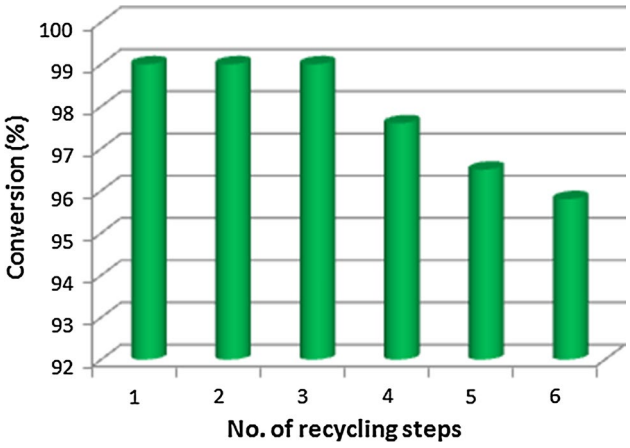

Fig. 7 Effect of recycling on the catalytic efficiency of PEDOT-NFs@Pd

Conclusion

An environmentally benign and highly efficient procedure for the C–C cross-coupling reactions of aryl halides with olefinic compounds has been developed under ultrasonic irradiation in water in the presence of PEDOT nanofibers/Pd(0) composites (PEDOT-NFs@Pd) as a new recyclable catalyst. High stability and reusability of catalyst, short reaction times, excellent yields, easy purification, very low palladium leaching and use of green solvent are main characteristics of this green catalytic process.

Acknowledgements We are grateful to University of Zanjan Research Council for partial support of this work.

References

1. J.H. Clark, Green Chem. **1**, 1–8 (1999)
2. C. Leonelli, T.J. Mason, Chem. Eng. Process. **49**, 885–900 (2010)
3. K. Ramachandran, T. Suganya, N. Nagendra Gandhi, S. Renganathan, Renew. Sust. Energy Rev. **22**, 410–418 (2013)
4. G. Cravotto, P. Cintas, Chem. Soc. Rev. **35**, 180–196 (2006)
5. M.R. Nabid, S.J.T. Rezaei, R. Ghahremanzadeh, A. Bazgir, Ultrason. Sonochem. **17**, 159–161 (2010)
6. S.J.T. Rezaei, Y. Bide, M.R. Nabid, Tetrahedron Lett. **53**, 5123–5126 (2012)
7. S.J. Tabatabaei Rezaei, M.R. Nabid, A. Yari, S.W. Ng, Ultrason. Sonochem. **18**, 49–53 (2011)
8. R. Breslow, Acc. Chem. Res. **24**, 159–164 (1991)
9. S. Minakata, M. Komatsu, Chem. Rev. **109**, 711–724 (2009)
10. M. Akizuki, T. Fujii, R. Hayashi, Y. Oshima, J. Biosci. Bioeng. **117**, 10–18 (2014)
11. K. Saïd, Y. Moussaoui, M. Kammoun, R.B. Salem, Ultrason. Sonochem. **18**, 23–27 (2011)
12. M. Bagherzadeh, M. Amini, P. Derakhshandeh, M. Haghdoost, J. Iran. Chem. Soc. **11**, 441–446 (2014)
13. S. Bhattacharjee, W.-S. Ahn, J. Nanosci. Nanotechnol. **15**, 6856–6859 (2015)
14. R.F. Heck, J.P. Nolley, J. Org. Chem. **37**, 2320–2322 (1972)
15. Z. Zhang, Z. Zha, C. Gan, C. Pan, Y. Zhou, Z. Wang, M.-M. Zhou, J. Org. Chem. **71**, 4339–4342 (2006)
16. C. Deraedt, D. Astruc, Acc. Chem. Res. **47**, 494–503 (2014)
17. J.A. Przyojski, K.P. Veggeberg, H.D. Arman, Z.J. Tonzetich, ACS Catal. **5**, 5938–5946 (2015)
18. Z. Donga, Z. Yea, Reusable Adv. Synth. Catal. **356**, 3401–3414 (2014)
19. C.S. Yeung, V.M. Dong, Chem. Rev. **111**, 1215–1292 (2011)
20. M.S. Cheung, F.K. Sheong, T.B. Marder, Z. Lin, Chem. Eur. J. **21**, 7480–7488 (2015)
21. Y. Lee, M.C. Hong, H. Ahn, J. Yu, H. Rhee, J. Organomet. Chem. **769**, 80–93 (2014)
22. N. Shang, S. Gao, X. Zhou, C. Feng, Z. Wang, C. Wang, RSC Adv. **4**, 54487–54493 (2014)
23. P. Taladriz-Blanco, P. Hervés, J. Pérez-Juste, Top. Catal. **56**, 1154–1170 (2013)
24. J. Lu, J.W. Elam, P.C. Stair, Acc. Chem. Res. **46**, 1806–1815 (2013)
25. M.A. Betiha, H.M.A. Hassan, E.A. El-Sharkawy, A.M. Al-Sabagh, M.F. Menoufy, H.E.M. Abdelmoniem, Appl. Catal. B: Environ. **182**, 15–25 (2016)
26. M. Hronec, K. Fulajtárová, I. Vávra, T. Soták, E. Dobročka, M. Mičušík, Appl. Catal. B: Environ. **181**, 210–219 (2016)
27. F. Pinna, Catal. Tod. **41**, 129–137 (1998)
28. C. Bara, E. Devers, M. Digne, A.F. Lamic-Humblot, G.D. Pirngruber, X. Carrier, ChemCatChem **7**, 3422–3440 (2015)
29. P. Munnik, P.E. de Jongh, K.P. de Jong, Chem. Rev. **115**, 6687–6718 (2015)
30. L. McMillan, L.F. Gilpin, J. Baker, C. Brennan, A. Hall, D.T. Lundie, D. Lennon, J. Mol. Catal. A: Chem. **411**, 239–246 (2016)
31. S. Xue, H. Jiang, Z. Zhong, Z.X. Low, R. Chen, W. Xing, Micropor. Mesopor. Mater. **221**, 220–227 (2016)
32. E. Taglauer, H. Knözinger, phys.Status.Solidi. b **192**, 465-475 (1995)
33. L. Groenendaal, F. Jonas, D. Freitag, H. Pielartzik, J.R. Reynolds, Adv. Mater. **12**, 481–494 (2000)
34. I.F. Perepichka, D.F. Perepichka, H. Meng, F. Wudl, Adv. Mater. **17**, 2281–2305 (2005)
35. T.K. Das, S. Prusty, Polym.-Plast. Technol. Eng. **51**, 1487–1500 (2012)
36. D. Astruc, F. Lu, J.R. Aranzaes, Angew. Chem. Int. Ed. **44**, 7852 (2005)
37. S. Vinod Selvaganesh, J. Mathiyarasu, K.L.N. Phani, V. Yegnaraman, Nanoscale Res. Lett. **2**, 546–549 (2007)
38. S. Harish, J. Mathiyarasu, K.L.N. Phani, V. Yegnaraman, Catal. Lett. **128**, 197–202 (2009)
39. V.K. Veniamin, A.B. Tatyana, G.T. Elena, J. Solid State Electrochem. **17**, 1621–1630 (2013)
40. M. Ilieva, V. Tsakova, W. Erfurth, Electrochim. Acta **52**, 816–824 (2006)
41. D. Sthitaprajna, N. Munichandraiah, Electrochim. Acta **180**, 339–352 (2015)
42. B.M. Choudary, M. Roy, S. Roy, M.L. Kantam, B. Sreedhar, K.V. Kumar, Adv. Synth. Catal. **348**, 1734 (2006)
43. S.J.T. Rezaei, Y. Bide, M.R. Nabid, Synth. Metal. **161**, 1414–1419 (2011)
44. M. Reza Nabid, S.J. Tabatabaei Rezaei, S. Zahra Hosseini, Mater. Lett. **84**, 128–131 (2012)
45. J. Zhu, J. Zhou, T. Zhao, X. Zhou, D. Chen, W. Yuan, Appl. Catal. A: Gen. **352**, 243–250 (2009)
46. L. Shao, Y. Ren, Z. Wang, C. Qi, Y. Lin, Polymer **75**, 168–177 (2015)
47. J.G. Benjamin, W.K. Robert, B.K. Richard, L.D. Paula, Angew. Chem. Int. Ed. **46**, 7251–7254 (2007)

48. M.R. Nabid, Y. Bide, S.J. Tabatabaei Rezaei, Appl. Catal. A: Gen. **406**, 124–132 (2011)
49. H. Ahmar, A.R. Fakhari, M.R. Nabid, S.J.T. Rezaei, Y. Bide, Sens. Actuat. B: Chem. **171–172**, 611–618 (2012)
50. H. Hosseini, S.J.T. Rezaei, P. Rahmani, R. Sharifi, M.R. Nabid, A. Bagheri, Sens. Actuat. B: Chem. **195**, 85–91 (2014)
51. B.E. Warren, *X-ray Diffraction* (Dover Publications Inc, New York, 1969)
52. M. Nabid, Y. Bide, E. Aghaghafari, S. Rezaei, Catal. Lett. **144**, 355–363 (2014)
53. G. Yang, Y. Zhou, H.-B. Pan, C. Zhu, S. Fu, C.M. Wai, D. Du, J.-J. Zhu, Y. Lin, Ultrason. Sonochem. **28**, 192–198 (2016)
54. M. Ghotbinejad, A.R. Khosropour, I. Mohammadpoor-Baltork, M. Moghadam, S. Tangestaninejad, V. Mirkhani, RSC Adv. **4**, 8590–8596 (2014)
55. R.R. Deshmukh, R. Rajagopal, K.V. Srinivasan, Chem. Commun. **17**, 1544–1545 (2001). doi:10.1039/B104532F